

## PHASE TRANSITION IN NUCLEAR SHAPE IN THE $A \approx 100$ REGION ?

J. Stachel, N. Kaffrell, N. Trautmann, Institut für Kernchemie, Universität Mainz  
H. Emling, H. Folger, E. Grosse, R. Kulesa<sup>+</sup>, D. Schwalm, GSI Darmstadt  
K. Brodén, G. Skarnemark, Department of Nuclear Chemistry, Chalmers University, Göteborg  
D. Eriksen, Department of Nuclear Chemistry, University Oslo

### Abstract

Two different types of experiments for the investigation of the neutron-rich Ru-isotopes are presented. A discussion of the neutron-rich isotopes of the  $A \approx 100$  transitional region is given in the framework of the Interacting Boson Model.

### 1. Introduction

After the discovery of well-deformed nuclei in the middle of the neutron-shell  $N = 82-126$  and around  $N = 140-150$  nearly thirty years ago, very soon a region of deformation was predicted also around the middle of the  $N = 50-82$  shell corresponding to a mass-number of  $A \approx 100$ . Subsequently various theoretical investigations<sup>1-5</sup> have been concerned with this mass-region and the results of different microscopic calculations point to a phase transition in nuclear shape between vibrational nuclei near the shell-closure  $N = 50$  and deformed shapes for the more neutron-rich nuclei. Following these calculations in the middle of the neutron-shell different types of deformation, prolate, oblate, triaxial or even shape coexistence between minima of different deformation seem to be possible.

To answer the question whether this predicted transition is realized in the nuclei of this mass-region, one has to investigate long isotope-chains starting from stable isotopes near  $N = 50$  up to extremely unstable isotopes near the middle of the neutron-shell with  $\beta^-$ -half-lives of only a few seconds.

The following discussion will be concerned mainly with the Ru-isotopes, since for these nuclei the experimental information covers now the whole region of interest.

Already the level energy systematics of the lowest excited states give some evidence for an increasing deformation; so the excitation energy  $E(2_1^+)$  of the  $2_1^+$ -state decreases continuously from  $\approx 650$  to  $\approx 240$  keV for  $^{98-110}\text{Ru}$ <sup>6-8</sup>. At the same time the ratio  $E(4_1^+)/E(2_1^+)$  rises from 2.14 to 2.76 and the  $B(E2, 2_1^+ \rightarrow 0_1^+)$ -value increases from  $\approx 20$  to 65 single particle units<sup>9-12</sup>.

To obtain more detailed information about the heavier Ru-isotopes we have chosen two different experimental techniques. In section 2 Coulomb excitation experiments of the stable isotopes  $^{102,104}\text{Ru}$  will be discussed, which yielded besides excitation energies and spins also  $B(E2)$ -values and diagonal E2-matrix elements (i.e. electric quadrupole moments). The unstable isotopes  $^{106,108}\text{Ru}$  have been studied observing the  $\gamma$ -radiation following the  $\beta^-$ -decay of the short-lived precursors  $36 \text{ s-}^{106}\text{Tc}$  and  $5 \text{ s-}^{108}\text{Tc}$ . Measurements of  $\gamma\gamma$ -coincidences and  $\gamma\gamma$ -angular correlations allowed the construction of level schemes, the assignment of spins and the determination of

E2/M1 mixing ratios. This will be discussed in section 3. Finally we will come back to the question, what one can learn from the experimental information gathered so far with respect to the supposed shape transition in section 4. For this purpose experimental data will be compared to a schematic study in the framework of the Interacting Boson Model.

### 2. Multiple Coulomb excitation of $^{102,104}\text{Ru}$

In previous Coulomb excitation experiments<sup>9,10</sup> using light ions ( $\alpha, ^{16}\text{O}$ ) the  $4_1^+$ -state in both  $^{102}\text{Ru}$  and  $^{104}\text{Ru}$  was reached. For the investigation of higher excited states and hence the identification of possible band-structures we used the  $^{208}\text{Pb}$  (4.6 MeV/u) beam of the UNILAC at Darmstadt to bombard thin targets of  $^{102}\text{Ru}$  and  $^{104}\text{Ru}$  ( $\approx 500 \mu\text{g}/\text{cm}^2$   $^{102,104}\text{Ru}$  on  $35 \mu\text{g}/\text{cm}^2$  C). The use of a special particle-gamma-coincidence set-up allowed for the correction of the strongly Doppler-broadened gamma-spectra observed with 3 Ge(Li)-detectors. Additional measurements of  $\gamma\gamma$ -coincidences using thick targets ( $\approx 2 \text{ mg}/\text{cm}^2$   $^{102,104}\text{Ru}$  on  $50 \text{ mg}/\text{cm}^2$   $^{208}\text{Pb}$ ) were performed to place the observed transitions in the level schemes of  $^{102,104}\text{Ru}$ . Both ground state band (gsb) and  $\gamma$ -band can be identified up to  $I^\pi = 8^+$ .

The measurement of  $\gamma$ -yields over a large range of scattering angles ( $64^\circ < \theta_{\text{cm}} < 147^\circ$ ) allowed the determination of E2-matrix elements (ME). For this purpose we used an iteration procedure<sup>13</sup>, which compares the experimental  $\gamma$ -yields with those obtained from a modified de Boer-Winther-Code starting from E2-ME resulting from different collective models, namely the Generalized Collective Model (GCM)<sup>14</sup>, the Interacting Boson Model (IBA-2)<sup>15</sup> and the Asymmetric Rotor+VMI Model (AR)<sup>16</sup>. To warrant model independent results one has to take into account all ME (mainly E2 but also M1, E1, E3, E4) connecting the observed states; especially the influence of their size and relative phase on the extracted E2-ME has to be tested carefully for all scattering angles.

It was shown<sup>17</sup>, that for the determination of  $B(E2)$ -values in a band it is useful to define yield ratios  $R_I(\theta) = Y_I(\theta)/Y_{I-2}(\theta)$ , where  $Y_I(\theta)$  is the  $\gamma$ -intensity of the transition from the state with spin  $I$  to the state with spin  $I-2$  at a scattering angle  $\theta$ . These yield ratios are mainly determined by the  $B(E2)$ -value for the corresponding transition. For the gsb-yields the influence of the other in-band transitions and the various interband transitions from the  $\gamma$ -band turns out to be roughly one order of magnitude weaker. Since most of these transitions are observed in the present experiment, these transition ME can be fixed by fitting the corresponding yield ratios. Amongst the remaining unknown ME the influence of the diagonal E2-ME  $\langle I || E2 || I \rangle$  on the gsb yield ratios plays the dominant role. To demonstrate this we show in fig. 1 experimental  $\gamma$ -yields together with the fitting result for two different diagonal ME for the  $6_1^+$ -state. Note, that their influence on the  $\gamma$ -yields is strong for small impact parameters, whereas for large impact parameters the  $\gamma$ -yields are especially sensitive to the corresponding E2-transition ME. Therefore one can extract both the  $B(E2)$ -values and

<sup>+</sup> On leave from Jagiellonian University, Cracow, Poland

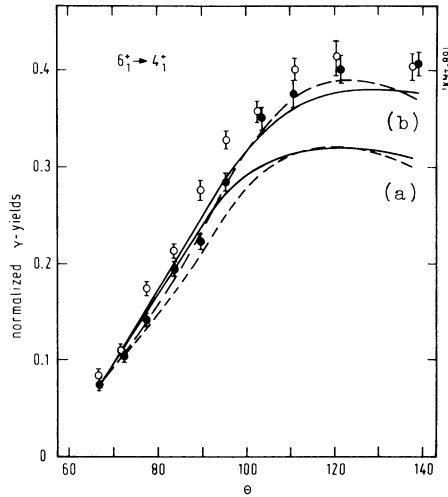


Fig. 1  $\gamma$ -ray yields for the  $6_1^+ \rightarrow 4_1^+$  transition normalized to the  $2^+ \rightarrow 0^+$  transition as a function of the scattering angle  $\theta_{cm}$ . The open circles (solid lines) correspond to events, where the  $\gamma$ -radiation is emitted along the recoil axis; for the closed circles (dashed lines) the relative angle between the  $\gamma$ -rays and the recoil axis was  $60^\circ$ . The curves represent the calculated yield-ratios assuming  $\langle 6_1^+ || E2 || 6_1^+ \rangle = -0.60$  eb (a) and  $\langle 6_1^+ || E2 || 6_1^+ \rangle = -0.36$  eb (b).

the electric quadrupole moments by fitting the experimental  $\gamma$ -yields. Note, that in order to reproduce the yields observed under different  $\gamma$ -angles deorientation effects have to be taken into account carefully. The deorientation coefficients were determined experimentally and were found to be rather strong especially for the  $2_1^+$ -state, which has a lifetime of 81 ps.

The resulting  $B(E2)$ -values for the gsb are shown in fig. 2a. For the  $10_1^+ \rightarrow 8_1^+$  transition no clear-cut assignment can be made. Nevertheless, one

can estimate an upper limit for the E2-strength, connecting the  $8_1^+$ -state with the next higher excited state(s); this estimate is based on the intensity and angular distribution of the  $8_1^+ \rightarrow 6_1^+$  transition assuming 960 keV for the  $10_1^+ \rightarrow 8_1^+$  transition energy. This is the value of the strongest unassigned  $\gamma$ -line in the spectrum; this energy is even above what one would expect from band systematics. Reducing this transition energy drastically (<100 keV) the corresponding  $10_1^+ \rightarrow 8_1^+$   $B(E2)$ -value reduces to about 40 % (lower limit of the error bar in fig. 2a). The  $B(E2, 2_1^+ \rightarrow 0_1^+)$ -value is the mean-value resulting from previous experiments<sup>9,10</sup>; for the  $4_1^+ \rightarrow 2_1^+$  transition the corresponding mean values shows to be in rather good agreement with our value. Also shown in fig. 2a are the gsb  $B(E2)$ -values as predicted by different collective nuclear models; For all these models the over-all agreement with the experiment is about the same.

Fig. 2b shows the corresponding diagonal E2-ME of the levels of the gsb. The rather strong decrease between the  $2_1^+$ - and  $4_1^+$ -value is the most striking feature, which can be reproduced quite well by the rigid triaxial rotor model (AR) using  $\beta = .275$  and  $\gamma = 25^\circ$  whereby the model parameters have been adjusted to the excitation energies and transition probabilities only. All other collective models predict a rather steep increase of the diagonal ME with increasing spin; also the  $O(6)$ -limit of the Interacting Boson Model<sup>23</sup>, which is equivalent to the Jean-Wilets  $\gamma$ -unstable Rotor Model<sup>24</sup>) can predict only a rather steep increase in the currently used form of the model. Indeed it is the spin-dependence of the quadrupole moments, which allows to distinguish clearly between the stiff-triaxial<sup>16</sup>) and the  $\gamma$ -unstable Rotor Model. The error bar for the  $8_1^+$  diagonal ME blows up in decreasing direction due to the large uncertainty of the  $B(E2, 10_1^+ \rightarrow 8_1^+)$ -value in direction to lower values.

### 3. Excited states in $^{106,108}\text{Ru}$

Since the neutron-rich isotopes  $^{106,108}\text{Ru}$  are unstable against  $\beta^-$ -decay they cannot be investigated by Coulomb excitation. So we have chosen the  $\beta^-$ -decay of their shortlived precursors  $36\text{ s } ^{106}\text{Tc}$  and  $5\text{ s } ^{108}\text{Tc}$  to feed excited states in these nuclei. The activity was produced by thermal neutron

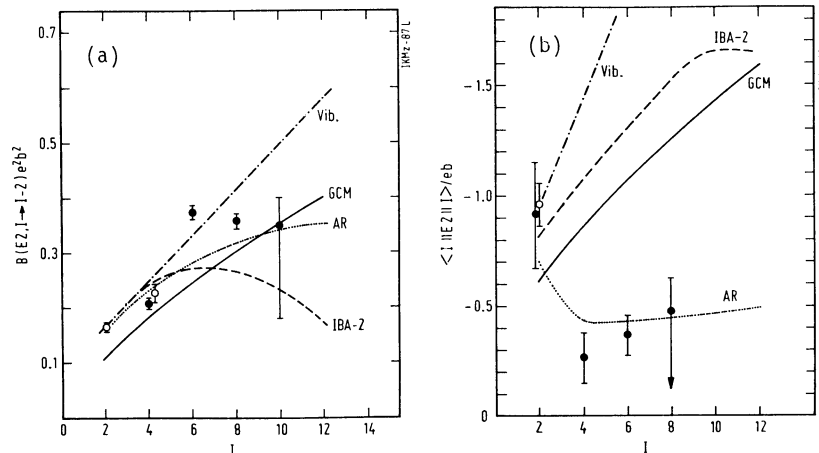


Fig. 2 (a)  $B(E2)$ -values for the gsb of  $^{104}\text{Ru}$ . The closed circles result from this experiment, the open circles are mean values of ref. 9 and 10. (b) Diagonal E2-ME for the gsb of  $^{104}\text{Ru}$  (closed circles: present experiment, open circle: mean value of ref. 10, 19-22). The different lines represent predictions of the Vibrational Model (Vib)<sup>18</sup>), the Generalized Collective Model (GCM)<sup>14</sup>), the Asymmetric Rotor Model (AR)<sup>16</sup>) and the Interacting Boson Model (IBA-2)<sup>15</sup>).

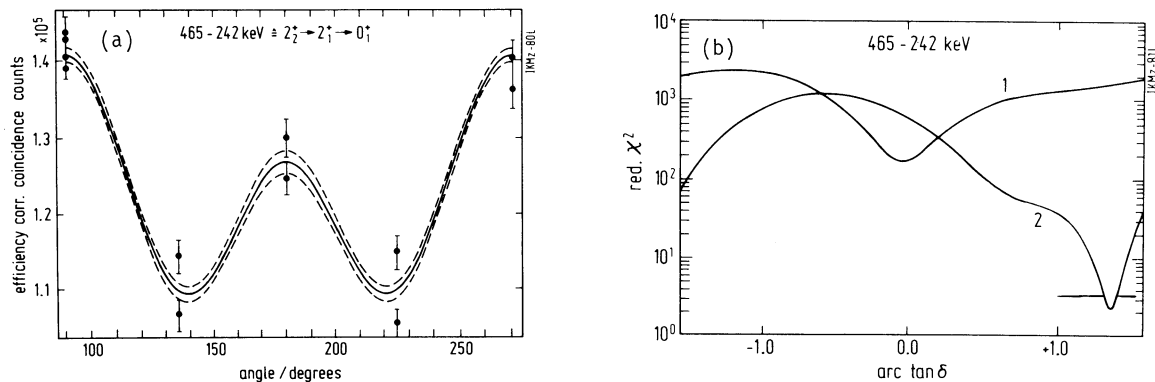


Fig. 3 (a)  $\gamma\gamma$ -angular correlation of the 465 keV - 242 keV cascade in  $^{108}\text{Ru}$ .  
 (b)  $\chi^2$  versus  $\arctan \delta$  plot for the 465 keV - 242 keV cascade and the two possible initial spin values; the horizontal line marks the statistical error for the accepted solution (spin 2).

induced fission of  $^{239}\text{Pu}$  in the Mainz TRIGA reactor. For a rapid on-line isolation of the Tc-activity from the fission product mixture we used the continuously working chemical separation system SISAK-II. This method consists of several mixer-centrifuge units and is based on a liquid-liquid extraction chemistry (for details see the contribution of N. Trautmann et al. to this conference or ref. 25).

In a first experiment the timing was optimized to measure the  $\gamma$ -radiation following the 36 s -  $^{106}\text{Tc} \rightarrow ^{108}\text{Ru}$   $\beta^-$ -decay. The activity reached the measuring position  $\approx 7$  s after fission with a continuous flux of  $\approx 10$  ml/s.

In order to keep the measuring cell small enough a 4 cm<sup>3</sup> polyethylene cell was filled with an anion-exchanger (DOWEX 1 x 4), which kept the Tc-activity for about 30 s in this measuring position. With 2 Ge(Li)-detectors both in a distance of 5 cm from the middle of the measuring cell  $\gamma\gamma\theta(t)$  coincidences have been measured for 5 different angles. Due to the finite source dimensions and solid angles re-

markable corrections were necessary; nevertheless, we obtain reliable results as can be demonstrated for the  $0_1^+ \rightarrow 2_1^+ \rightarrow 0_1^+$  cascade, where the experimental coefficients  $A_{22} = 0.34$  (9) and  $A_{44} = 1.20$  (16) are in rather good agreement with the theoretical ones (0.3571 and 1.1429).

To obtain similar information about  $^{108}\text{Ru}$  with a 5 s half-life precursor, the SISAK system was reduced to 2 mixer-centrifuge units; this enabled the start of measurement  $\approx 5$  s after fission. To suppress longer-lived activities the measuring time was shortened to about 1 s; the Tc-activity fluxed with  $\approx 12$  ml/s through a polyethylene cell (diameter 2 cm, length 4 cm). So we could measure comparable activities of  $^{106}, ^{107}, ^{108}\text{Tc}$  with 3 Ge(Li)-detectors.

The level schemes of  $^{106}\text{Ru}$  and  $^{108}\text{Ru}$  have been studied previously by measurements of  $\gamma\gamma$ -coincidences using the same separation technique<sup>8</sup>). In the case of  $^{108}\text{Ru}$  the much better statistics allowed us, to construct numerous additional excited levels. As is the case for  $^{102}\text{Ru}$  and  $^{104}\text{Ru}$  also for  $^{106}, ^{108}\text{Ru}$  the head of a gsb ( $0^+, 2^+, 4^+$ ) and a  $\gamma$ -band ( $2^+, 3^+, (4^+)$ ) can be identified. Levels with higher spin values are not fed in allowed  $\beta^-$ -decay since the precursors  $^{106}, ^{108}\text{Tc}$  have relatively low ground state spins ( $1^\pi = 2^+, 3^+$ )<sup>26</sup>).

Fig. 3a shows a typical  $\gamma\gamma$ -angular correlation. Via a  $\chi^2$ -minimisation procedure we can make spin assignments for most of the observed levels and determine multipole mixing ratios for the stronger transitions. For an example see fig. 3b. In  $^{106}\text{Ru}$  most of the excited states above 2 MeV have spin values of  $I = 1$  and presumable negative parity, since their decay to the  $2_1^+$ -state is predominantly dipole radiation; the nature of these states is still unclear. The until now missing first excited  $0^+$ -state in  $^{108}\text{Ru}$  could be located only  $\approx 1$  keV above the  $3_1^+$ -state through a 20 % admixture of its characteristic 0-2-0 angular correlation to the  $3_1 \rightarrow 2_1 \rightarrow 0_1$  cascade.

Some of the resulting E2/M1 mixing ratios are shown in table 1 together with the corresponding values for  $^{102}, ^{104}\text{Ru}$ . As is expected for transitions between collective bands the transitions between gsb and  $\gamma$ -band show a predominant E2-character with rather weak M1-contributions (<10 %). On the other hand the  $2_3^+$ -state decays mainly by M1-radiation, which does not fit in the collective picture and hence can not be reproduced by the used collective

Table 1

E2/M1-mixing ratios  $\Delta$  ( $\Delta = \langle I_f || E2 || I_i \rangle / \langle I_f || M1 || I_i \rangle$  - unit eb/ $\mu_n$  - with  $\Delta = \delta / .835 \cdot E_\gamma$  (MeV)) of some  $\gamma$ -transition in  $^{102-108}\text{Ru}$ . The values for  $^{102}\text{Ru}$  and  $^{104}\text{Ru}$  are taken from ref. 27 and 7.

	$^{102}\text{Ru}$	$^{104}\text{Ru}$	$^{106}\text{Ru}$	$^{108}\text{Ru}$
$2_2^+ \rightarrow 2_1^+$	$-114 \pm 38$	$-81^{+31}_{-121}$	$17.9^{+4.8}_{-2.2}$	$11.1^{+2.2}_{-1.6}$
$3_1^+ \rightarrow 2_1^+$	$-8.4 \pm 0.7$	$-4.3 \pm 0.5$	$-6.2^{+1.6}_{-1.8}$	$-3.0^{+0.5}_{-0.8}$
$4_2^+ \rightarrow 4_1^+$	-	$4.1^{+6.6}_{-1.8}$	-	-
$2_3^+ \rightarrow 2_1^+$	$0.27 \pm 0.03$	$0.45 \pm 0.12$	$0.28 \pm 0.15$	$1.03^{+.66}_{-.46}$

models. As will be discussed in section 4 also the interpretation of the  $0^+$ -state, which is connected to this  $2_3^+$ -state, is difficult within these models.

#### 4. Discussion of the $A \approx 100$ region in the framework of the IBA-1

In the following the  $A \approx 100$  transitional region will be discussed in the Interacting Boson Model<sup>31)</sup> (here in its simplest form, which does not distinguish between proton and neutron bosons, the so-called IBA-1). Its three dynamical symmetries<sup>32-34)</sup>, the SU(5)-, SU(3)- and O(6)-limit correspond to the three geometrical descriptions of nuclei as anharmonic vibrators, rigid axialsymmetric rotors<sup>18)</sup> and soft triaxial rotors<sup>24)</sup>. Moreover the full IBA-1 Hamilton operator describes all direct and complex transitions between these limiting cases in a consistent and relatively simple way. The symmetry triangle in fig. 4 shows this in a symbolic way.

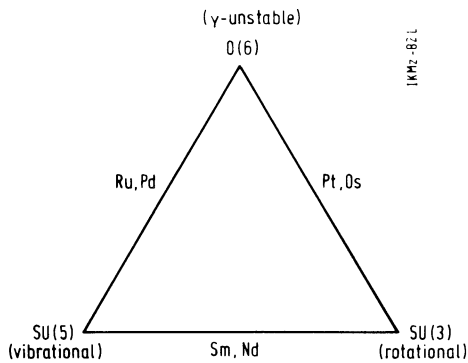


Fig. 4 Symmetry triangle symbolizing the three dynamical symmetries of the IBA-1 and the possible transitions between them. The transition SU(5)  $\rightarrow$  SU(3) is realized in the Nd/Sm-nuclei<sup>28)</sup>, the transition SU(3)  $\rightarrow$  O(6) in the Pt/Os-nuclei<sup>29)</sup>.

Now the question arises, where on this triangle can the  $A \approx 100$  transitional region be located. As already mentioned, in the Ru-isotopes the energy ratio  $E(4_1^+)/E(2_1^+)$  increases continuously with increasing neutron number starting from a vibrational value near the shell closure at  $N = 50$ , but it stays clearly below the rotational value of 3.3 also for the heaviest of the known isotopes. For the Zr-, Mo- and Pd-isotopes ( $Z = 40, 42, 46$ ) a similar trend is observed; The increase is rather steep between  $N = 58$  and 60 for the Zr- and Mo nuclei and rather moderate for the Pd-isotopes. In fig. 5 the  $B(E2, 2_1^+ \rightarrow 0_1^+)$ -values for Ru/Pd-isotopes are shown in comparison to those of Nd-isotopes, representing a transition from vibrational to rotational nuclei (SU(5)  $\rightarrow$  SU(3)<sup>28)</sup> and of Os-isotopes, representing a transition from rotational to  $\gamma$ -unstable nuclei (SU(3)  $\rightarrow$  O(6)<sup>29)</sup>. Although two different shells are compared, for the  $A \approx 100$  region a transition between SU(5)- and O(6)-nuclei is suggested; a comparison of some experimental B(E2)-ratios with the model predictions for the three limits confirms this suggestion (table 2); in any case a transition towards the SU(3)-limit can be excluded. For this

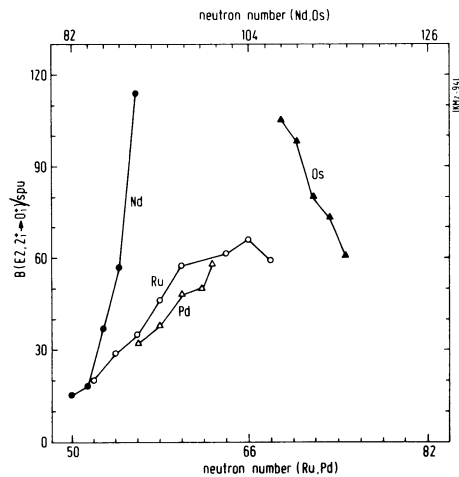


Fig. 5 Experimental B(E2)-values for the  $2_1^+ \rightarrow 0_1^+$  transition in Ru-<sup>9-12</sup>), Pd-<sup>35-38</sup>), Nd-<sup>39</sup>) and Os-isotopes<sup>40,41)</sup> in single particle units.

transition one would expect also a rather sudden onset of deformation connected to discontinuities for the SU(5)  $\rightarrow$  SU(3) transition<sup>30)</sup>.

Since, until now, no examples are known for the SU(5)  $\rightarrow$  O(6) transition, a more detailed discussion seems to be worthwhile. In the following we will briefly outline a schematic study of this transition. It is convenient to write the IBA-1 Hamiltonian for this purpose in a multipole expansion of s- and d-boson creation and annihilation operators<sup>31)</sup>:

$$H = \epsilon n_d + \kappa P \cdot P + \kappa' L \cdot L + \kappa'' Q \cdot Q + a_3 T_3 \cdot T_3 + a_4 T_4 \cdot T_4 \quad (1)$$

For the SU(5)-limit the monopole term  $\epsilon n_d$  is dominant, while for the O(6)-limit the pairing term  $\kappa P \cdot P$  is the most important. Thus for a study of the SU(5)  $\rightarrow$  O(6) transition one should vary the ratio of these two terms systematically. Neglecting the other terms in the Hamiltonian, the corresponding simpli-

Table 2

B(E2)-ratios for low-lying excited states as resulting from the three IBA-1 limits; in comparison the corresponding experimental values for <sup>102-108</sup>Ru are shown<sup>7,9,10,42-45)</sup>.

B(E2)-ratios	$\frac{2_2 \rightarrow 0_1}{2_2 \rightarrow 2_1}$	$\frac{2_2 \rightarrow 2_1}{2_1 \rightarrow 0_1}$	$\frac{3_1 \rightarrow 2_1}{3_1 \rightarrow 4_1}$	$\frac{4_2 \rightarrow 4_1}{4_2 \rightarrow 2_2}$	$\frac{4_1 \rightarrow 4_1}{2_2 \rightarrow 2_1}$
SU(5)	.011	1.40	.06	.72	1.0
SU(3)	.70	.02	2.50	.03	6.93
O(6)	.07	.79	.12	.75	1.84
<sup>102</sup> Ru	.036(3)	.71(7)	.18(2)	.51	1.62(21)
<sup>104</sup> Ru	.045(4)	.86(7)	.10(2)	.54(5)	1.57(17)
<sup>106</sup> Ru	.087(11)	--	.16(7)	--	--
<sup>108</sup> Ru	.103(11)	--	.21(6)	--	--

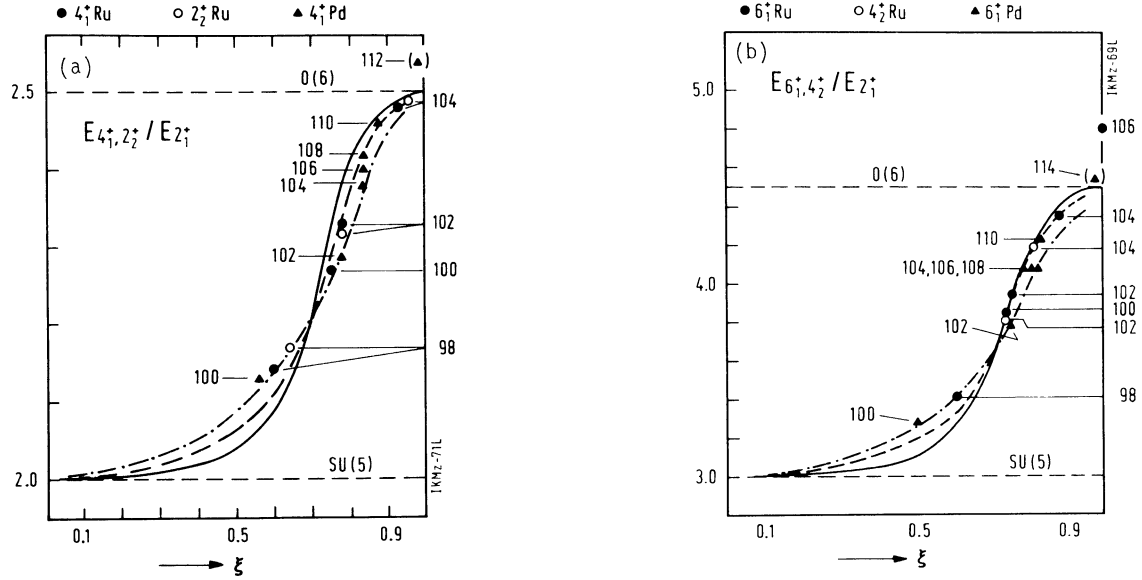


Fig. 6 (a,b) Calculated relative excitation energy of the  $4_1^+/2_2^+$ - and  $6_1^+/4_2^+$ -states in dependence of  $\xi$  for three different total boson numbers  $N$  (full line for  $N = 14$ , dashed line for  $N = 8$ , dashed-dotted line for  $N = 5$ ). The experimental values for Ru- and Pd-isotopes<sup>6,7,42,46,47</sup>) are marked on the corresponding curves or interpolated between them.

fied Hamiltonian can be written as

$$H = \epsilon(d^{\dagger}\tilde{d})^{(0)} + \kappa(d^{\dagger}d^{\dagger} - s^{\dagger}s^{\dagger})^{(0)} \cdot (\tilde{d}\tilde{d} - ss)^{(0)} \quad (2)$$

This formalism was also chosen by Dieperink et al.<sup>30</sup>) in their investigation of the changes in ground-state properties connected with the shape phase transitions in the Interacting Boson Model. The treatment of the  $SU(5) \rightarrow O(6)$  transition using only one free parameter  $\kappa/\epsilon$  is certainly a rather drastic simplification, but the characteristic features of the phase transition are expected<sup>30</sup>) to be contained in this description.

In fig. 6a,b we compare the experimental excitation energies for several low-lying excited states ( $4_1^+$ ,  $2_2^+$ ,  $6_1^+$ ,  $4_2^+$ ) with the theoretical ones resulting from these IBA-1 calculations. This is done for different total boson numbers  $N(N=5, 8, 14)$  as a function of  $\xi = \eta/1+\eta$  with  $\eta = 4\kappa/\epsilon(N-1)^{30}$ ). In this parametrization the phase transition occurs exactly at  $\xi = 0.5$  for  $N = \infty$ , but is smeared out for smaller boson numbers. The comparison of theory and experiment gives  $\xi$ -values of 0.5 - 1.0 for the Ru- and Pd-isotopes. In the case of Pd, only the energy of the  $4_1^+$ -state was considered, as the  $2_2^+$ -state is not at the same energy experimentally in contradiction to this simplified IBA-description.

The decay properties only depend partly on  $\xi$ . The ratio  $B(E2, 4_1^+ \rightarrow 2_1^+)/B(E2, 2_1^+ \rightarrow 0_1^+)$  e.g. does not change characteristically between the two limits under consideration; therefore it does not help for the localization of the Ru/Pd-isotopes in the  $SU(5) \rightarrow O(6)$  transitional region. On the other hand some transitions which are forbidden in the  $SU(5)$ -limit as cross-over transitions, increase by several orders of magnitude with increasing  $\xi$  and reach the observed experimental values for the  $2_2^+ \rightarrow 0_1^+$ ,  $3_1^+ \rightarrow 2_1^+$  and  $4_2^+ \rightarrow 2_1^+$ -transition at  $\xi = 0.5 - 1.0$ . Again for Ru  $\xi$  rises with the neutron number, while for Pd this trend is not so clear, and even is in the opposite direction for some cases.

Thus as far as excitation energies and  $B(E2)$ -ratios are concerned in the Ru-isotopes we seem to

observe a continuous development from nearly vibrational nuclei ( $^{96,98}\text{Ru}$ ) to nuclei with a well pronounced  $O(6)$ -character ( $^{106,108}\text{Ru}$ ). The known Pd-isotopes can be located clearly on the  $O(6)$ -side of this phase transition.

There are two distinct deviations from this simple picture. For the  $SU(5) \rightarrow O(6)$  transition a very characteristic feature is the change in the decay mode of the  $0_2^+$ -state, since the  $SU(5)$ -limit allows an  $E2$ -decay only to the  $2_1^+$ -state, whereas in the  $O(6)$ -limit only a transition to the  $2_2^+$ -state is possible. The experimental situation in the  $A \approx 100$  region appears to be rather complex: on the one hand the  $0_2^+$ -states in the Ru/Pd-nuclei are rather low in energy, more resembling a two-phonon triplet, and no decay to the  $2_2^+$ -state is observed; on the other hand the experimental ratio  $B(E2, 0_2^+ \rightarrow 2_1^+)/B(E2, 2_1^+ \rightarrow 0_1^+)$ <sup>9,10,42,35</sup>) is about a factor of 2-3 smaller than the  $SU(5)$ -prediction. Moreover these  $0_2^+$ -states are populated in (t,p) reactions leading to  $^{104,106}\text{Ru}$ <sup>48</sup>) with  $\approx 20\%$  of the ground-state population, while this is forbidden in the  $SU(5)$ - as well as in the  $O(6)$ -limit<sup>49</sup>).

As mentioned above, also the predominant  $M1$ -decay of the  $2_3^+$ -state rules out the interpretation of the  $0_2^+$ ,  $2_3^+$ -sequence in a simple collective picture. This leads to the conclusion, that the experimental  $0_2^+$ -states in the Ru/Pd-nuclei may not be the IBA  $0_2^+$ -states. In fact in some cases ( $^{106,108,110}\text{Pd}$ ,  $^{102}\text{Ru}$ ) second excited  $0^+$ -states are known<sup>6</sup>), which show the expected dominant decay to the  $2_2^+$ -state<sup>27,43,50-53</sup>).

Concerning the real origin of the experimental  $0_2^+$ -states, different suggestions have been made: phenomena such as shape coexistence between minima of different deformation or large  $2p$ - $2n$  admixtures (protons as neutrons) have been discussed already for Cd-, Sn- and Zr- isotopes<sup>54-57</sup>) as well as for  $^{102-110}\text{Pd}$ <sup>58,59</sup>). The enhancement observed in two neutron transfer reactions<sup>48,60</sup>) would favour the latter interpretation (two neutron correlated states).

The other discrepancy occurs in the spin-depen-

dence of the quadrupole moments as discussed in section 2. The experimental results are surprisingly well reproduced by the rigid triaxial rotor model. IBA-calculations performed so far (this investigation and ref. 15) are in disagreement with the experiment in this point. On the one hand the case of a rigid triaxial rotor is not contained in an IBA Hamiltonian limited to one- and two-body terms. On the other hand, a rigid triaxial rotor cannot explain the  $0_2^+$  properties.

#### References:

- 1) D.A. Arseniev, A. Sobiczewski, V.G. Soloviev, Nucl. Phys. A139, 269 (1969)
- 2) I. Ragnarsson, Proc. Int. Conf. on properties of nuclei far from the region of beta-stability, Leysin, 1970, CERN 70-30, p. 847
- 3) W. Fabian, G.E.W. Horlacher, K. Albrecht, Nucl. Phys. A190, 533 (1972)
- 4) A. Faessler, J.E. Galonska, U. Götz, H.C. Pauli, Nucl. Phys. A230, 303 (1974)
- 5) D. Bucurescu, G. Constantinescu, M. Ivascu, Rev. Rom. Phys. Tome 24, No. 10, 941, Bucarest, 1979
- 6) C.M. Lederer, V.S. Shirley, Table of Isotopes, 7th ed., New York, 1978
- 7) K. Sümmerer, N. Kaffrell, N. Trautmann, Nucl. Phys. A308, 1 (1978)
- 8) K. Sümmerer, N. Kaffrell, N. Trautmann, K. Brodén, G. Skarnemark, T. Björnstad, I. Haldorsen, J.A. Maruhn, Nucl. Phys. A339, 74 (1980)
- 9) F.K. McGowan, R.L. Robinson, P.H. Stelson, W.T. Milner, Nucl. Phys. A113, 529 (1968)
- 10) S. Landsberger, R. Lecomte, P. Paradis, S. Monaro, Phys. Rev. C21, 588 (1980)
- 11) R.C. Jared, H. Nifenecker, S.G. Thompson, Proc. 3. Symp. on Physics and Chemistry of Fission, Rochester, IAEA 1974, Vol. 2, p. 211
- 12) E. Cheifetz, H.A. Selic, A. Wolf, R. Chechik, J.B. Wilhelmy, Nucl. Spectroscopy of Fission Products, Workshop ILL, Grenoble, 1979
- 13) H. Ower, Ph. D. thesis, Univ. Frankfurt, 1980, and to be published
- 14) G. Gneuss, W. Greiner, Nucl. Phys. A171, 449 (1971); P. Hess, J.A. Maruhn, private communication
- 15) F. Iachello in Interacting Boson in Nuclear Physics ed. by F. Iachello, Plenum Press, New York, 1979, p. 1; P. van Isacker, G. Puddu, Nucl. Phys. A348, 125 (1980)
- 16) A.S. Davydov, G.F. Filippov, Nucl. Phys. 8, 237 (1958); H. Toki, A. Faessler, Z. Phys. A276, 35 (1976)
- 17) E. Grosse, A. Bajtanda, H. Emling, F. Folkmann, P. Fuchs, R.B. Piercey, D. Schwalm, H.J. Wollersheim, D. Evers, H. Ower, Phys. Scripta, in print
- 18) A. Bohr, B.R. Mottelson, Nucl. Structure, W.A. Benjamin Inc., Reading, 1975, Vol. 2
- 19) P.H. Stelson, Adv. Nucl. Phys. 1, 1 (1968)
- 20) M.F. Nolan, I. Hall, D.J. Thomas, M.J. Throop, J. Phys. A6, L57 (1973)
- 21) M. Maynard, D.C. Palmer, J.R. Cresswell, P.D. Forsyth, I. Hall, D.G.E. Martin, J. Phys. G3, 1735 (1977)
- 22) C. Fahlander, L. Hasselgren, G. Possnert, J.E. Thun, Phys. Scripta 18, 47 (1978)
- 23) A. Arima, F. Iachello, Phys. Rev. Lett. 40, 385 (1978)
- 24) L. Wilets, M. Jean, Phys. Rev. 102, 788 (1956)
- 25) K. Brodén, G. Skarnemark, T. Björnstad, D. Eriksen, I. Haldorsen, N. Kaffrell, E. Stender, N. Trautmann, J. inorg. nucl. Chem. 43, 765 (1981)
- 26) G. Tittel, Ph. D. thesis, Univ. Mainz, 1980
- 27) B. Singh, H.W. Taylor, Nucl. Phys. A155, 70 (1970)
- 28) O. Scholten, F. Iachello, A. Arima, Ann. Phys. 115, 325 (1978)
- 29) R.F. Casten, J. Cizewski, Nucl. Phys. A309, 477 (1978)
- 30) A.E.L. Dieperink, O. Scholten, Nucl. Phys. A346, 125 (1980)
- 31) Interacting Bosons in Nuclear Physics, ed. F. Iachello, Plenum Press, New York, 1979
- 32) A. Arima, F. Iachello, Phys. Rev. Lett. 35, 1069 (1975)
- 33) A. Arima, F. Iachello, Ann. Phys. 99, 253 (1976)
- 34) A. Arima, F. Iachello, Phys. Rev. Lett. 40, 385 (1978)
- 35) R.L. Robinson, F.K. McGowan, P.H. Stelson, W.T. Milner, R.O. Sayer, Nucl. Phys. A124, 553 (1969)
- 36) A. Christy, I. Hall, R.P. Harper, I.M. Naqib, B. Wakefield, Nucl. Phys. A142, 591 (1970)
- 37) R.P. Harper, A. Christy, I. Hall, I.M. Naqib, B. Wakefield, Nucl. Phys. A162, 161 (1971)
- 38) J. Lange, A.T. Kandil, J. Neuber, C.D. Uhlhorn, H. v. Buttler, A. Bokisch, Nucl. Phys. A292, 301, (1977)
- 39) P.H. Stelson, L. Grodzins, Nucl. Data 1, 21 (1965)
- 40) R.F. Casten, J.S. Greenberg, S.H. Sie, G.A. Burginyon, D.A. Bromley, Phys. Rev. 187, 1532 (1969)
- 41) W.T. Milner, F.K. McGowan, R.L. Robinson, P.H. Stelson, R.O. Sayer, Nucl. Phys. A177, 1 (1971)
- 42) J. Stachel, N. Kaffrell, H. Emling, H. Folger, E. Grosse, R. Kulessa, D. Schwalm, to be published.
- 43) D. De Frenne, H. Thierens, E. Jacobs, P. De Gelder, P. D'hondt, A. De Clercq, K. Heyde, A.J. Deruytter, Phys. Rev. C18, 486 (1978)

- 44) A. Bockisch, M. Miller, A.M. Kleinfeld, Z. Physik A292, 265 (1979)
- 45) J. Stachel, N. Kaffrell, N. Trautmann, K. Brodén, G. Skarnemark, D. Eriksen, to be published
- 46) H. Bohn, priv. communication
- 47) L. Hasselgren, J. Srebrny, C.Y. Wu, D. Cline, T. Czosnyka, R.M. Diamond, D. Habs, H. Hübel, H. Körner, U. Smilansky, F.S. Stephens, G.R. Young, C. Baktash, Rochester Annual Report 1979
- 48) R.F. Casten, E.R. Flynn, O. Hansen, T.J. Mulligan, Nucl. Phys. A184, 357 (1972)
- 49) A. Arima, F. Iachello, Phys. Rev. C16, 2085 (1977); J.A. Cizewski, E.R. Flynn, R.E. Brown, J.W. Sunier, Phys. Lett. 88B, 207 (1979) and ref. cited therein
- 50) J. Konijn, E.W.A. Lingeman, F. Diederix, B.J. Meijer, P. Koldewijn, A.A.C. Klaasse, Nucl. Phys. A138, 514 (1969)
- 51) R.J. Gehrke, R.G. Helmer, Phys. Rev. 177, 1792 (1969)
- 52) S.T. Hsue, H.H. Hsu, F.K. Wohn, W.R. Western, S.A. Williams, Phys. Rev. C12, 582 (1975)
- 53) L.I. Govor, A.M. Demidov, I.B. Shkalov, M.R. Ahmed, Kh.I. Shakavchi, S.A.-Najjar, M.A. Al-Amili, N. Al-Assafi, Nucl. Phys. A245, 14 (1975)
- 54) H.W. Fielding, R.E. Anderson, C.D. Zafiratos, D.A. Lind, F.E. Cecil, H.H. Wiemann, W.P. Alford, Nucl. Phys. A218, 389 (1977)
- 55) R.A. Meyer, L. Peker, Z. Physik A283, 379 (1977)
- 56) A. Bäcklin, N.-G. Jonsson, R. Julin, J. Kantele, M. Luontama, A. Passoja, T. Poikolainen, Nucl. Phys. A351, 490 (1981)
- 57) T.A. Khan, W.D. Lauppe, K. Sistemich, H. Lawin, G. Sadles, H.A. Selic, Z. Physik A283, 105 (1977); A284, 313 (1978)
- 58) H.H. Hsu, S.A. Williams, F.K. Wohn, F.J. Margetan, Phys. Rev. C16, 1626 (1977)
- 59) L. Hasselgren, D. Cline, Proc. Conf. on Interacting Bose-Fermi-Systems in Nuclei, Erice, Sicily 1980, Pergamon Press, 1980
- 60) R.E. Anderson, J.J. Kraushaar, I.C. Oelrich, R.M. Delvecchio, R.A. Naumann, E.R. Flynn, C.E. Moss, Phys. Rev. C15, 123 (1977)

#### DISCUSSION

*A. Gelberg:* While I consider the evidence for a shape transition as very convincing, one should be rather prudent as far as the  $SU(5) \rightarrow O(6)$  transition is concerned. 1) It is not easy to distinguish between the two limits, at least for the lowest bands. 2) Can there be an  $SU(5)$  symmetry in a nucleus with 6  $\pi$ -holes and 4... $\nu$ -particles? 3) In this situation it is generally difficult to assign a definite symmetry.

*J. Stachel:* 1) I agree that in general it is not easy to distinguish between the  $SU(5)$  and the  $O(6)$  limit. But as I showed, some properties change in a very characteristic way, even if there is not such a sharp transition as between  $SU(5)$  and  $SU(3)$ . 2) and 3) A comparison of the experimental data in Ru-isotopes with the schematic study of the  $SU(5) \rightarrow O(6)$  transition shows that there are no purely vibrational nuclei, the lightest isotopes ( $^{96,98}\text{Ru}$ ) seem to be placed around  $\xi = 0.5$ , which is just the region of the so-called phase transition (onset of deformation). The Pd-isotopes seem all to be located on the  $O(6)$  side of this transitional region and no clear neutron-number dependence is observed.

*C. Baktash:* From your quadrupole moment values, it seems that the data prefers a rigid- $\gamma$  core. From our experience in the Os-Pt region, the matrix elements of the quasi-gamma band are also very sensitive to the softness of the core with respect to the  $\gamma$ -vibrations. Could you comment if these matrix elements in your data prefer soft- or rigid- $\gamma$  cores?

*J. Stachel:* As far as E2-matrix elements determined from our Coulomb excitation experiment (transition between the even members of the  $\gamma$ -band and inter-band transitions between these states and the ground state band) are concerned, there is no significant difference between  $\gamma$ -soft calculations (IBA) and  $\gamma$ -rigid ones (Toki-Faessler). This might have to do with the fact that in the  $\gamma$ -rigid calculations  $\gamma$  was chosen  $25^\circ$ , which gives the best fit to excitation energies and transition probabilities; in the  $\gamma$ -unstable limit of the IBA ( $O(6)$ )  $\gamma$  has a dynamical mean value of about  $30^\circ$ . This means that from our data one cannot distinguish between a static and a dynamic  $\gamma$ -deformation around  $25$ - $30^\circ$ , except if one takes into consideration the quadrupole moments.